Journal of Macromolecular Science, Part A
Publication details, including instructions for authors and subscription information:
http://www.informaworld.com/smpp/title~content=t713597274

Physicochemical Study of Cationic Polybis(1-indenyl)

P. Nicolet[a]
[a] Laboratoire de Physique, Pharmaceutique Institut des Sciences Médicales, Algérie

To cite this Article Nicolet, P.(1977) 'Physicochemical Study of Cationic Polybis(1-indenyl)', Journal of Macromolecular Science, Part A, 11: 3, 577 — 602
To link to this Article: DOI: 10.1080/00222337708061289
URL: http://dx.doi.org/10.1080/00222337708061289

J. MACROMOL. SCI.–CHEM., A11(3), pp. 577-602 (1977)

Physicochemical Study of Cationic Polybis(1-indenyl)

P. NICOLET

Laboratoire de Physique Pharmaceutique
Institut des Sciences Médicales d'Alger
Alger, Algérie

ABSTRACT

We have carried out a study of polybis(1-indenyl) obtained by cationic polymerization. For this purpose we used GPC, light scattering, viscometry, and DTA. We compared the real distribution with the log-normal function. We established the value of the Mark-Houwink coefficients. We have shown the existence of important branching and opened up discussions on their origin. We have also shown that the ratio $A_2M_w/[\eta]$ stays constant in spite of the branching.

INTRODUCTION

Among the numerous products derived from indene synthesized by Marechal and his collaborators [1-7], bis(1-indenyl) has a very special place. It is effectively the only diene in which the two ethylenic bonds are near enough to one another to be able to interact with each other during polymerization. The obtainment of polymer of high molecular weight but of low intrinsic viscosity proved the necessity of a more detailed study on the distribution curves and structures of polybis(1-indenyl).

We therefore undertook a study of the molecular weight distribution by analytic gel-permeation chromatography (GPC) and we obtained by preparative GPC samples of low dispersion necessary for a study by light scattering and viscometry.

We tried to get some information on the shape of molecular chains, particularly the importance and nature of the branching. For this purpose we measured the molecular weight, the reciprocal particle scattering factor, the intrinsic dissymmetry, the second virial coefficient, the radius of gyration, and the intrinsic viscosity of fractionated samples. We showed the possibility of postpolymerization reactions by differential thermal analysis (DTA); this proved very useful for the interpretation of certain results.

EXPERIMENTAL

Gel-Permeation Chromatography

For preparative GPC, a Chromatoprep 100 instrument from Waters Associates was used. The solvent was benzene at room temperature. The detector was an R 400 differential refractometer from Waters Associates thermostatted to better than 0.01°C. Three columns of internal diameter of 5 cm, length 1.20 m, of permeabilities 5×10^3, 1.5×10^4, and 7×10^5 Å were used.

Analytic GPC was performed with an ALP/GPC 501 instrument from Waters Associates. Permeabilities of the columns were in the range between 80 Å and 7×10^5 Å.

Light Scattering

Scattered light was measured by an Fica 4000 instrument. The solutions were centrifuged for 2 hr at 15,000 rpm to remove the dust. The solvent was benzene at 25°C.

Viscometry

Viscosities were defined by the use of Ubbelohde tubes placed in an automatic Hewlett-Packard instrument. The solvent was benzene at 25°C.

Differential Thermal Analysis

Thermograms were obtained by means of a Du Pont instrument.

RESULTS

The syntheses of the monomer and its cationic polymerization were described previously, as was a detailed study of the refractive index increment [8].

We shall keep in mind that we considered two modes of propagation of the polymerization reaction. The main one is associated with the simultaneous breaking of the two ethylenic bonds with the formation of a cyclobutane ring for each link. The secondary one would consist in the scission of only one ethylenic bond, leading to the appearance of an indenyl group as a side group. This preferential order is due to the consideration that the opposite order would probably give insoluble polymers, by analogy with the polymerization of the bis(6-indenyl) [9].

In addition to the branches having residual ethylenic bonds as an origin, one may also expect branches due to the attack of a benzene ring of the polymer by the carbocation of a growing chain.

The study of the physicochemical properties dealt with two samples described in Table 1.

FE was polymerized under conditions similar to those for FD, though at a slightly lower temperature and for a slightly longer time.

Preparative GPC Fractionation

The results are given in Tables 2 and 3.

We notice immediately that the distribution index of FE is twice that of FD. In other respects, if we compare the curves plotted in Fig. 1 which shows the percent by weight of the fractions versus the extraction number, we note that the curve for FE is wider than that for FD, in agreement with the distribution indexes; the fractions FE 3 and FE 4 are abnormally rich; the fractions FE 8 to FE 11 are abnormally poor. Thus, one must expect to find branching in the polybis(1-indenyl), particularly in the fractions of FE with high molecular weights.

The integral and differential distribution curves FD and FE are plotted in Figs. 2 and 3, respectively.

TABLE 1. Polymerization of Samples FD and FE

	Sample FD	Sample FE
Experimental conditions		
Initial concn of bis(1-indenyl) (mole/liter)	0.125	0.125
Initial concn of $TiCl_4$ (mole/liter)	0.01	0.01
Polymerization temperature (°C)	-70	-72
Polymerization time (min)	6	10
Polymer		
Conversion (%)	100	100
Yield (soluble fraction) (%)	100	99.8
$[\eta]$ (dl/g)	0.28	0.44
$\bar{M}_w \times 10^{-6}$	0.36	1.63

In the case of FD, these curves have a typical appearance, showing particularly for the differential curve a clear maximum near $[\eta] = 0.18$, followed by a regular decrease.

On the other hand, in the case of FE, we can see a drawing out of the integral curve towards the high values of $[\eta]$ and a flat maximum of the differential curve from 0.22 to 0.37 dl/g. This confirms the disappearance of polymer of medium viscosity in favor of relatively high viscosity polymer.

Analytical GPC Study

The instrument was first calibrated by use of commercial samples of linear polystyrene; then the "universal calibration curve" thus obtained was converted into specific curves for our samples FD and FE through the Mark-Houwink equation:

$$[\eta] = KM^{\alpha}$$

the coefficients of which were previously established.

TABLE 2. Results of Fractionation of FD[a]

Fraction	Weight (mg)	Weight (%)	Cumulative weight (%)	$[\eta]$ (dl/g)	$\bar{M}_w \times 10^{-6}$
FD 1	14.4	0.51	100	0.70	3.06
FD 2	43.9	1.57	99.49	0.67	2.12
FD 3	83.2	2.97	97.92	0.60	1.51
FD 4	124.4	4.44	94.95	0.55	1.31
FD 5	171.5	6.13	90.51	0.47	0.826
FD 6	213.3	7.62	84.83	0.42	0.589
FD 7	245.9	8.78	76.76	0.35	0.434
FD 8	269.8	9.64	67.98	0.31	0.321
FD 9	277.2	9.90	54.34	0.25	0.217
FD 10	271.7	9.70	48.44	0.22	0.158
FD 11	252.6	9.02	38.74	–	–
FD 12	221.4	7.91	29.72	–	–
FD 13	183.1	6.54	21.81	–	–
FD 14	139.7	4.99	15.27	–	–
FD 15	104.2	3.72	10.28	–	–
FD 16	77.8	2.78	6.56	–	–
FD 17	51.8	1.85	3.78	–	–
FD 18	32.8	1.17	1.93	–	–
FD 19	15.7	0.56	0.76	–	–
FD 20	5.6	0.20	0.20	–	–

[a]Flow rate, 34.2 ml/min; fraction volume, 171 ml; injected weight, 2.805 g in 250 ml of benzene; fractionation yield, 100%; calculated: $[\eta] = 0.28$ dl/g; $\bar{M}_w/\bar{M}_n = 2.5$; $\bar{M}_w = 0.37 \times 10^6$; $\bar{M}_n = 0.15 \times 10^6$, $\bar{M}_v = 0.29 \times 10^6$.

TABLE 3. Results of Fractionation of FE[a]

Fraction	Weight (mg)	Weight (%)	Cumulative weight (%)	$[\eta]$ (dl/g)	$\bar{M}_w \times 10^{-6}$
FE 1	3.24	0.085	100	1.61	21.8
FE 2	27.38	0.728	99.915	1.35	15.6
FE 3	95.81	2.550	99.187	1.23	9.24
FE 4	187.97	5.003	96.637	1.09	6.54
FE 5	225.63	6.006	91.634	0.93	4.76
FE 6	215.60	5.739	85.628	0.77	2.93
FE 7	239.89	6.386	79.889	0.65	2.26
FE 8	261.01	6.949	73.503	0.58	1.57
FE 9	298.32	7.942	66.554	0.50	1.22
FE 10	313.63	8.350	58.612	0.44	0.889
FE 11	309.94	8.252	50.262	0.37	0.648
FE 12	302.90	8.064	42.010	0.33	0.475
FE 13	283.18	7.539	33.946	0.27	0.296
FE 14	244.11	6.499	26.407	0.23	0.193
FE 15	202.75	5.398	19.908	0.20	0.140
FE 16	167.82	4.468	14.510	0.16	0.111
FE 17	126.54	3.369	10.042	0.13	0.102
FE 18	91.96	2.448	6.673	0.09	0.092
FE 19	62.22	1.656	4.225	–	–
FE 20	41.27	1.090	2.569	–	–
FE 21	25.61	0.682	1.470	–	–
FE 22	15.58	0.415	0.788	–	–
FE 23	9.15	0.244	0.373	–	–
FE 24	3.78	0.101	0.129	–	–
FE 25	1.06	0.028	0.028	–	–

[a]Flow rate, 35.2 ml/min; fraction volume, 176 ml; injected weight, 3.618 g in 250 ml of benzene; fractionation yield, 100%; calculated: $[\eta] = 0.47$ dl/g; $\bar{M}_w/\bar{M}_n = 5.2$; $\bar{M}_w = 1.62 \times 10^6$; $\bar{M}_n = 0.31 \times 10^6$; $\bar{M}_v = 1.0 \times 10^6$.

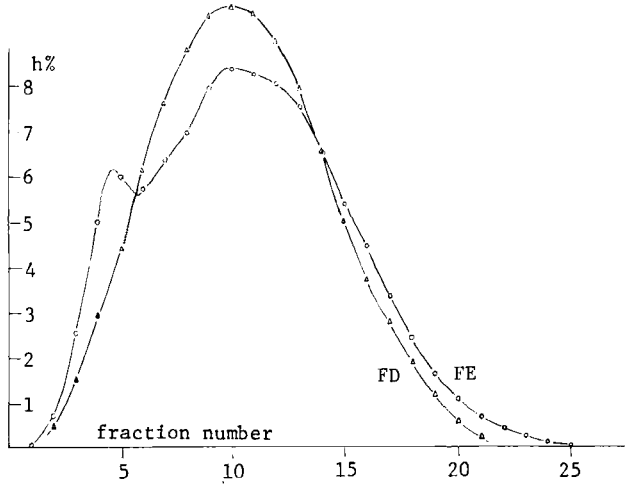

FIG. 1. Weight % h of FD and FE fractions as a function of their extraction number.

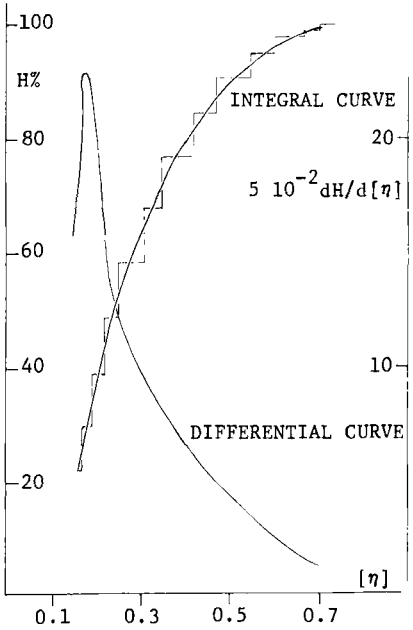

FIG. 2. Integral and differential distribution curves of FD as a function of the intrinsic viscosity (H denotes cumulative % weight; $[\eta]$ is in units of dl/g.

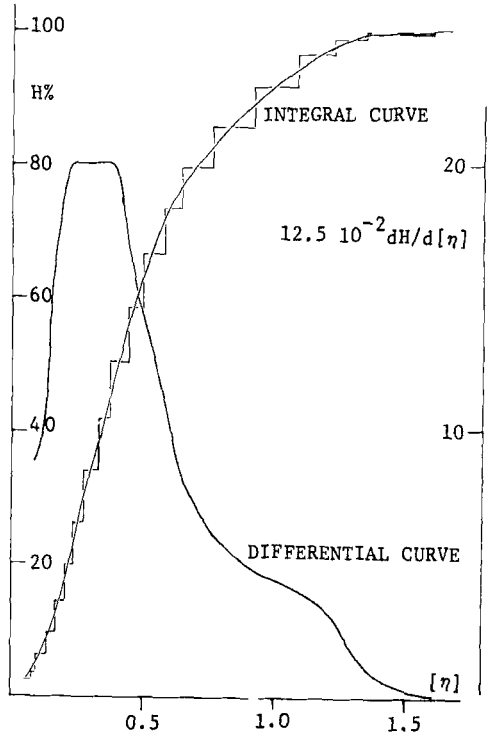

FIG. 3. Integral and differential distribution curves of FE as a function of the intrinsic viscosity.

TABLE 4. Analytical GPC Data

	$\overline{M}_w \times 10^{-6}$	$\overline{M}_n \times 10^{-6}$	$\overline{M}_v \times 10^{-6}$	$\overline{M}_w/\overline{M}_n$
FD	0.482	0.0288	0.233	16.7
FE	1.92	0.0359	0.840	53.7

Analytical GPC data are shown in Table 4 and the elution curves are plotted in Fig. 4.

In both cases, the comparison with the measured results (Table 1) shows a slight increase of $\overline{M}_w$, a marked decrease of $\overline{M}_n$ and consequently a much larger distribution index.

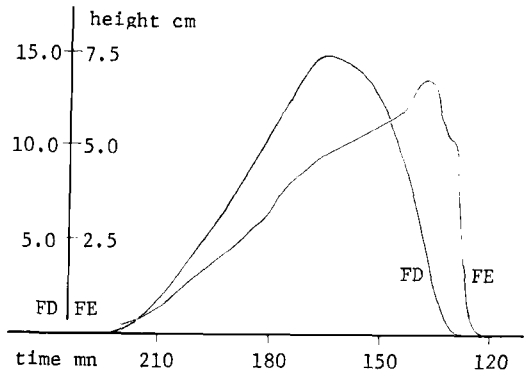

FIG. 4. Analytic GPC elution curves of FD and FE.

The data calculated from the fractions of preparative GPC were, on the contrary, much closer to the measured values, (Tables 2 and 3). Such differences have already been noticed and reported [11].

Distribution Function

We compared the distribution of FD and FE with the log-normal distribution function:

$$W(M) = dh_i/dM$$

$$= (1/\beta\sqrt{\pi})\,(1/M)\,e^{(-1/\beta^2 \ln M/M_0)}$$

for which the average molecular weights are:

$$\overline{M}_w = M_0 e^{\beta^2/4}$$

$$\overline{M}_n = M_0 e^{-\beta^2/4}$$

$$\overline{M}_v = M_0 e^{\alpha\beta^2/4}$$

The log-normal function shows a maximum:

$$M_{max} = M_0 e^{-\beta^2/2} < \overline{M}_n < \overline{M}_w$$

In other respects, the integral function

$$I(M) = \int_0^M W(M)dM$$

takes the specific value

$$I(M_0) = 0.5$$

Let us notice too, the specific value of the log-normal function:

$$W(M_0) = 1/M_0$$

The value of β has been determined through the equation:

$$\beta = \sqrt{(2)(2.303)\log \overline{M}_w/\overline{M}_n}$$

Then it is easy to calculate M_0.

The comparison between the data in Tables 5 and 6 indicates the log-normal distribution function represents the real distributions fairly well.

TABLE 5. Analytical GPC Data of FD (β = 2.37 and $M_0 = 0.118 \times 10^6$)

Log-normal function	Real distribution
$M_{max} = 0.007 \times 10^6$	$M_{max} = 0.006 \times 10^6$
$W(M_0) = 1.2 \times 10^{-6}$	$W(M_0) = 1.5 \times 10^{-6}$
$I(M_0) = 0.50$	$I(M_0) = 0.48$

TABLE 6. Analytical GPC Data of FE (β = 2.82 and M = 0.262×10^6)

Log-normal function	Real distribution
$M_{max} = 0.005 \times 10^6$	$M_{max} = 0.004 \times 10^6$
$W(M_0) = 0.43 \times 10^{-6}$	$W(M_0) = 0.5 \times 10^{-6}$
$I(M_0) = 0.50$	$I(M_0) = 0.48$

Light Scattering Study

Table 7 shows light scattering data. They will be compared in the following paragraphs.

Second Virial Coefficient A_2 as a Function of $\overline{M}_w$

The plot of A_2 versus $\overline{M}_w$ is shown in Fig. 5. The values of A_2 are low and may even become negative, which shows that benzene is a poor solvent for the polybis(1-indenyl). The shape of the two curves shows branching in the fractions with high molecular weights. The Fraction FD 4 seems to be rather more linear than the others (this will also be confirmed by other findings).

Reciprocal Particle-Scattering Factor $P^{-1}(90)$ as a Function of Intrinsic Dissymmetry [z]

The plot of $P^{-1}(90)$ versus [z] (Fig. 6) shows that the random coil is fairly representative of the polybis(1-indenyl) structure. However the experimental curves are at first above and then below the curve random coils; this may be explained by variation in A_2.

Radius of Gyration ρ as a Function of [z]

The study of the experimental curves (Fig. 7) leads to the same conclusions as above.

Reciprocal Particle-scattering Factors $P^{-1}(\theta)$ as a Function of Angle θ

We calculated the values of $P^{-1}(\theta)$ versus $\sin^2 \theta/2$ for the first 13 fractions of FE and we drew the curves for fractions FE 1, 2, 5, and 13 (Fig. 8). Taking into account the previously found structure for the

TABLE 7. Light-Scattering Data

Fraction	$A_2 \times 10^5$	$P^{-1}(90)$	$[z]$	ρ_o (Å)	First Cassassa ratio $A_2 M_w/[\eta]$ (mole)	Second Cassassa ratio $[\eta] M_w/\rho^3$ $\times 10^{10}$	Third Cassassa ratio $A_2 M_w^2/\rho^3$ $\times 10^{11}$ (mole)
FD 1	-18.3	1.51	1.62	501	–	0.0141	–
FD 2	5.2	1.47	1.45	479	1.55	0.0111	0.156
FD 3	6.3	1.35	1.38	424	2.30	0.0104	0.163
FD 4	8.8	1.53	1.34	626	1.84	0.0033	0.074
FD 5	10.7	1.24	1.32	452	1.81	0.0081	0.149
FD 6	12.3	1.23	1.24	338	1.58	0.0069	0.125
FD 7	12.8	1.20	1.22	320	1.59	0.0046	0.073
FD 8	17.4	1.21	1.19	326	1.22	0.0028	0.045
FD 9	15.3	1.16	1.17	282	1.40	0.0024	0.040
FD 10	19.7	1.10	1.12	213	1.64	0.0034	0.048
FE 1	-41.6	6.17	4.70	1487	–	0.0138	–
FE 2	0	3.61	3.44	1112	–	0.0152	–
FE 3	1.42	2.52	2.63	884	1.07	0.0164	0.175
FE 4	2.75	2.08	2.26	730	1.48	0.0187	0.275

FE 5	3.74	1.74	1.88	609	1.64	0.0179	0.294
FE 6	3.70	1.66	1.74	565	1.22	0.0137	0.165
FE 7	6.05	1.54	1.58	516	1.88	0.0106	0.201
FE 8	6.50	1.47	1.48	478	1.38	0.0078	0.108
FE 9	6.95	1.46	1.47	462	1.66	0.0057	0.095
FE 10	6.96	1.36	1.38	426	1.30	0.0048	0.063
FE 11	9.56	1.31	1.36	394	1.58	0.0039	0.063
FE 12	12.4	1.19	1.24	331	1.48	0.0040	0.058
FE 13	15.4	1.18	1.22	300	1.34	0.0020	0.030

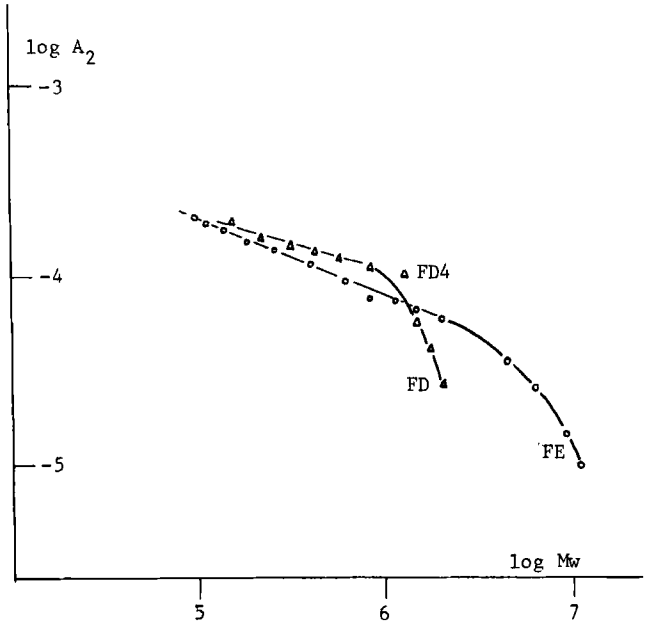

FIG. 5. Variation of log A_2 with log $\overline{M}_w$.

polybis(1-indenyl), we must attribute the asymptotic shape of the curves to the existence of important branchings in FE 1 and FE 2.

Radius of Gyration as a Function of $\overline{M}_w$

We can distinguish three zones in Fig. 9. For $0.13 < \overline{M}_w \times 10^{-6} < 0.32$, the variation seems to be linear and it might correspond to slightly branched chains, as the slope is very close to 0.5. For $0.32 < \overline{M}_w \times 10^{-6} < 3.2$, the points are placed on a downward-sloping curve, which is an indication of branching. We notice that with equal molecular weights, the radii of gyration of the fractions FD are lower than those of the fractions of FE, which seem less branched in this precise zone. For $\overline{M}_w \times 10^{-6} > 3.2$, the points again lie on a line which is parallel to the first one. However the chains cannot be linear, and the interpretation seems to be very

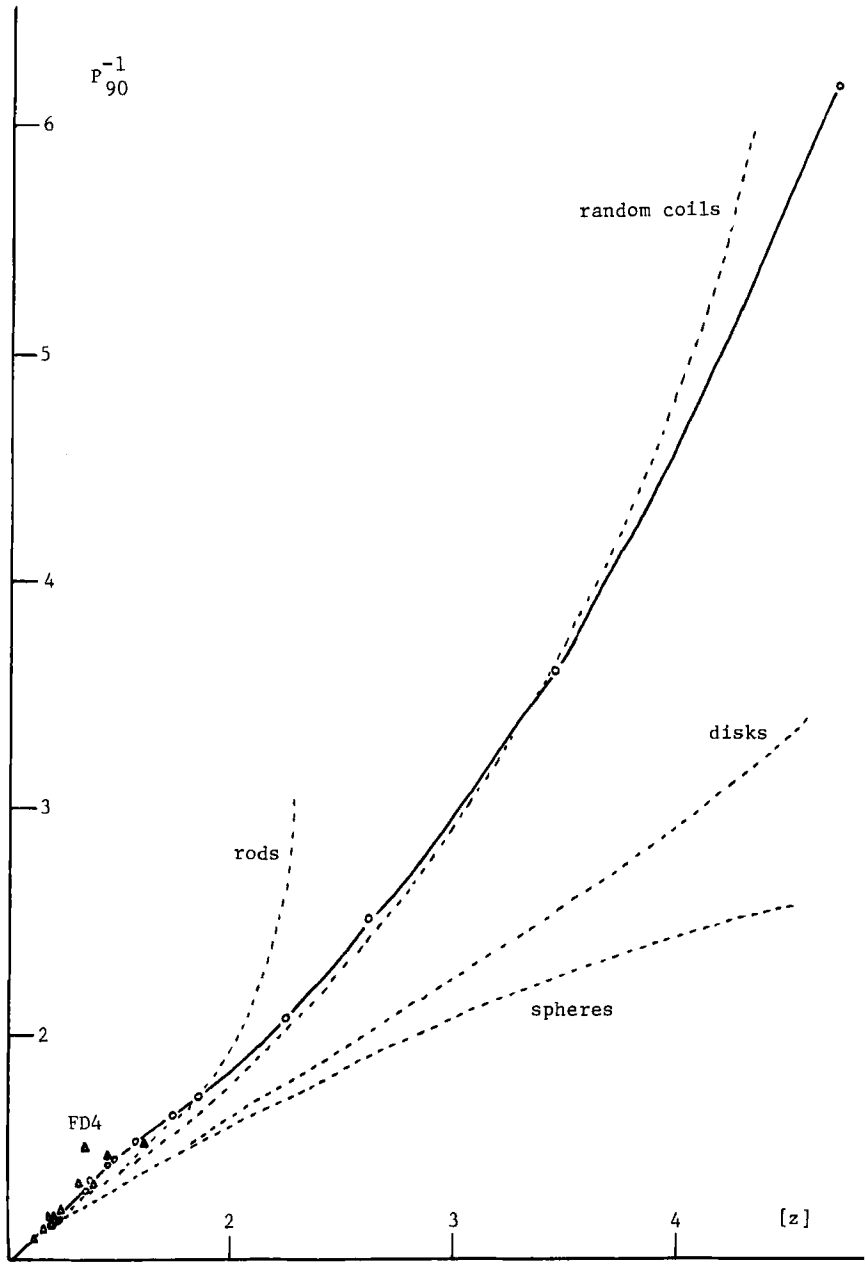

FIG. 6. Reciprocal of the particle-scattering factor $P^{-1}(90)$ as a function in intrinsic dissymmetry: (△) FD; (○) FE.

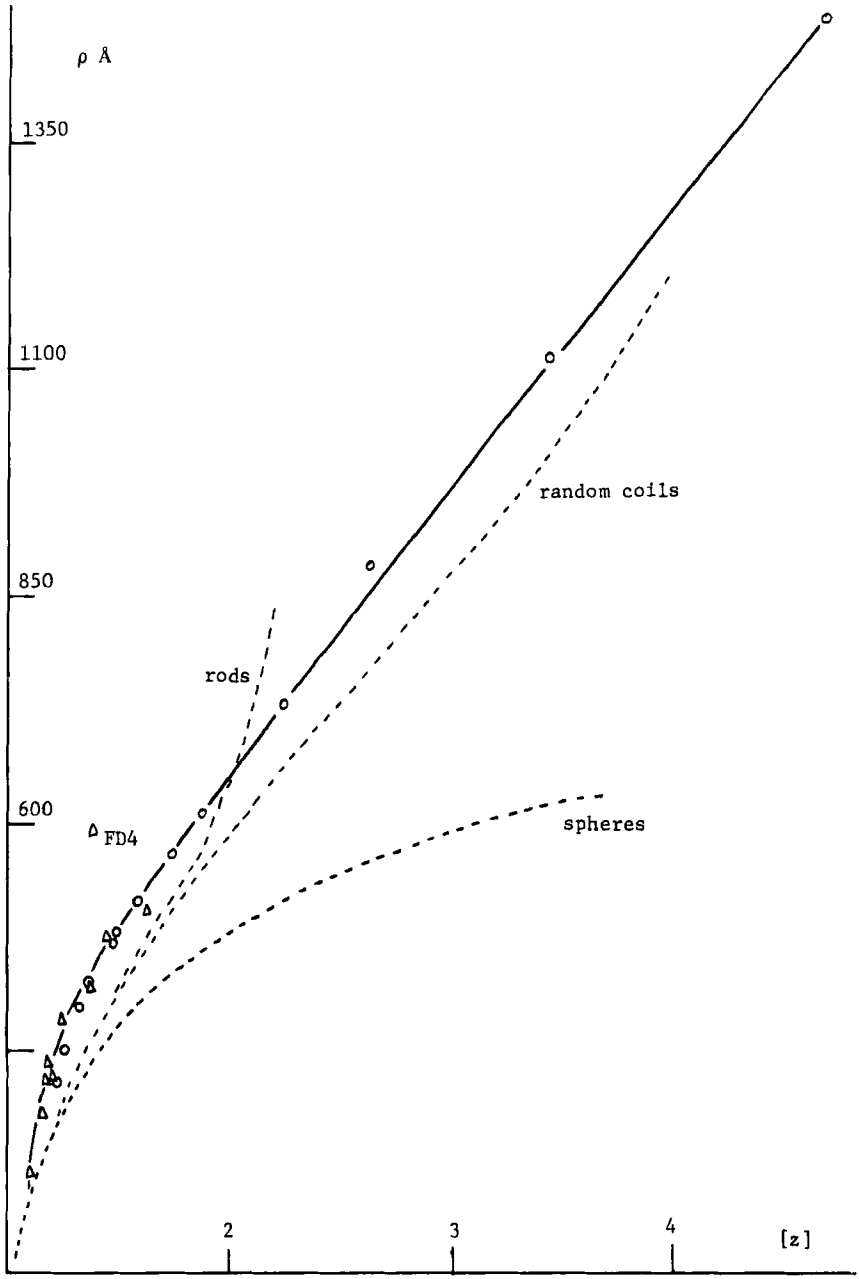

FIG. 7. Radius of gyration as a function of intrinsic dissymmetry: (△) FD; (○) FE.

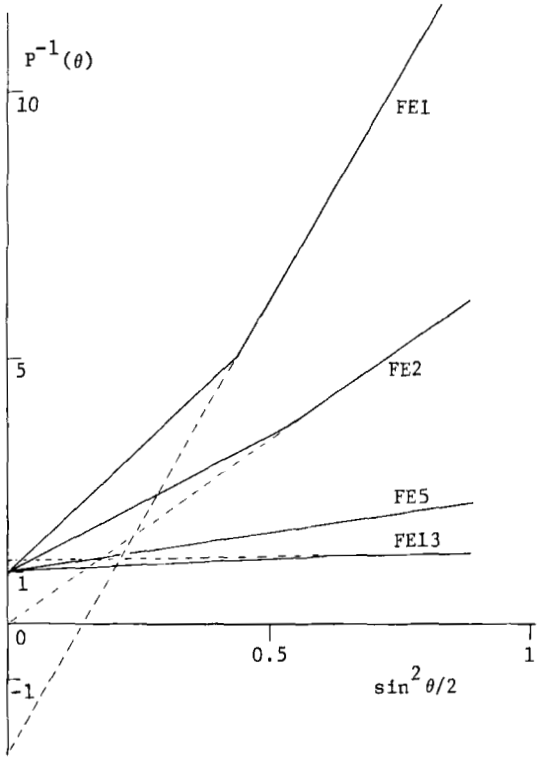

FIG. 8. Reciprocal of the particle-scattering factors $P^{-1}(\theta)$ as a function of angle θ for FE 1, FE 2, FE 5, and FE 13.

delicate. At best, we notice the analogy with the behavior of ring chains.

Study of Physicochemical Aggregates

We wanted to confirm that the polybis(1-indenyl) did not form aggregates in benzene at 25°C. To this effect, we operated upon three factors: the dilution, the increase of the temperature, and the impoverishment of the solvent. None of these changes, within experimental limits, showed a significant change of the molecular weight

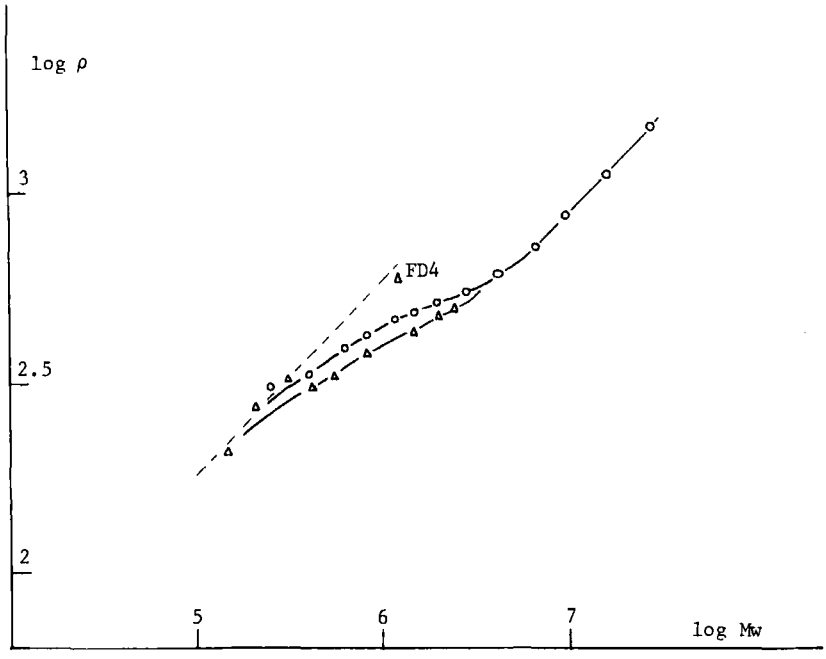

FIG. 9. Variation of log ρ (in Angstroms) with log $\overline{M}_w$: ($\triangle$) FD; ($\circ$) FE.

Dilution

The data for FE 7, such as $\overline{M}_w$, ρ, and A_2, remain constant within the limit of experimental error when the concentration varies in the ratio from 1 to 1/200.

Temperature

The average molecular weight of FE 3 is the same (± 3%) at 65°C and 25°C.

Solvent

Light scattering data of one sample ($\overline{M}_w = 0.39 \times 10^6$) in benzene, then in mixtures of isorefractive solvents such as ethylene bromide

TABLE 8. Influence of the Solvent on Light-Scattering Data

Solvent at 25°C	$M_W \times 10^{-6}$	ρ (Å)	$A_2 \times 10^5$
Benzene	0.400	367	13.8
EB (100%)	0.397	383	16.0
EB/BA, 95/5	0.410	374	–
EB/BA, 90/10	0.408	358	14.3
EB/BA, 80/20	0.380	333	9.6
EB/BA, 60/40	0.376	283	7.1
EB/BA, 40/60	0.391	272	5.1
EB/BA, 32/68	0.370	238	3.1

(EB) and benzyl alcohol (BA) are shown in Table 8. Here too, the variation of the average molecular weight is less than 5% (within the experimental error), in spite of the very clear impoverishment of the solvent, characterized by the lowering of A_2 in proportion of 5.

The variation of ρ with A_2 has also been plotted in Fig. 10. As shown by Outer, Carr, and Zimm [12], the extrapolation of the curve to zero A_2 allows us to assess the specific size of the molecules of the sample, due to a "skeletal" effect and characteristics of the chain rigidity.

Viscometric Study

In Fig. 11 the variation of log $[\eta]$ with log $\overline{M}_w$ is plotted (Tables 2 and 3). For fractionation of FD, all the points lie on the same straight line, for which we calculate the equation:

$$[\eta]\ (\mathrm{dl/g}) = 13 \times 10^{-4} \overline{M}_w^{0.43}$$

For fractionation of FE (for the linear portion) we calculate

$$[\eta]\ (\mathrm{dl/g}) = 9.2 \times 10^{-4} \overline{M}_w^{0.45}$$

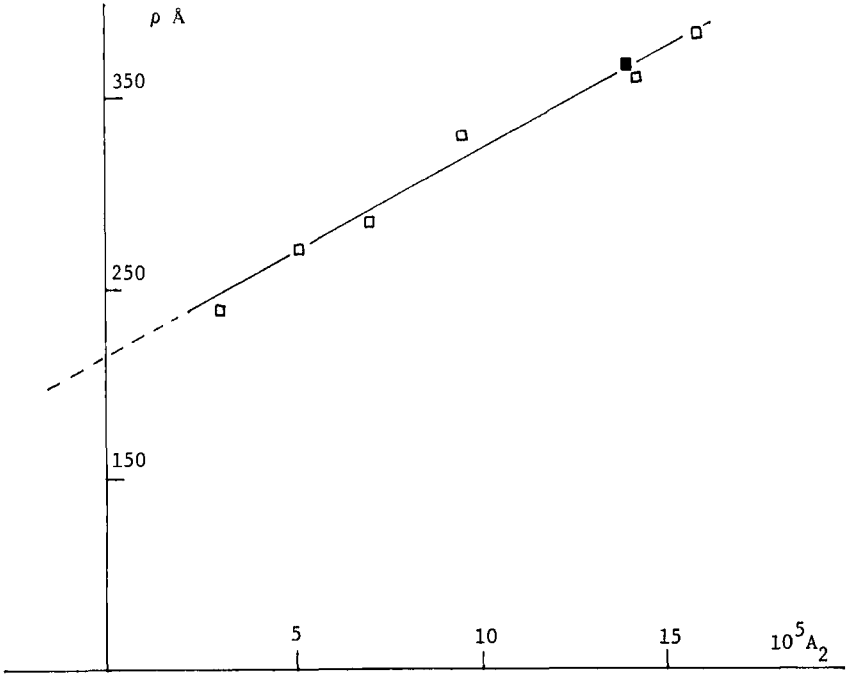

FIG. 10. Influence of the solvent on plots of radius of gyration vs. second virial coefficient: (■) C_6H_6; (□) $C_2H_4Br_2$–$C_6H_5CH_2OH$.

Fractions FE 1, FE 2, and FE 3 lie on a downward curve, which is a confirmation of their high degree of branching. On the other hand we notice that α for FD is slightly smaller than α for FE.

Cassassa [13] found that the ratios $A_2\overline{M}_w/[\eta]$, $A_2\overline{M}_w{}^2/\rho^3$, and $[\eta]\,\overline{M}_w/\rho^3$ ratios must be constant for a linear polymer. We calculated them in the case of polybis(1-indenyl), and we notice (Table 7) that only $A_2\overline{M}_w/[\eta]$ stays quite constant in spite of the branchings, the average value being 1.5 mole.

The variations of the two other ratios are plotted in Fig. 12. We clearly see that the branchings of FE fractions appear only for higher molecular weights but become more important than in the case of the FD fractions, which confirms all our previous results.

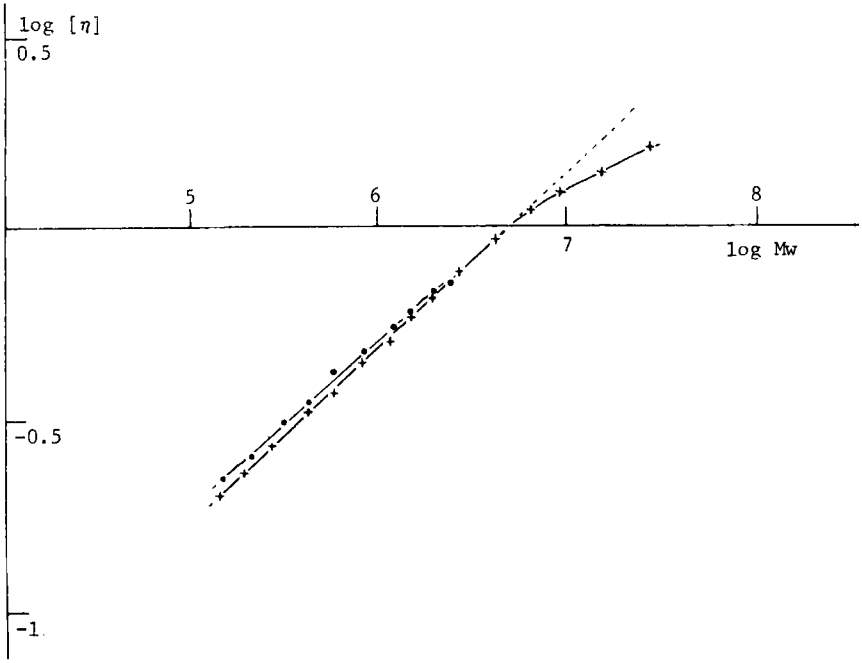

FIG. 11. Variation of log $[\eta]$ with log $\overline{M}_w$: (•) FD; (+) FE.

For comparison, we calculated the Cassassa ratios for the poly-4, 7-dimethylindene and for the poly-6-methylindene [14]. For poly-4, 7-dimethylindene (for which branchings were found): $A_2\overline{M}_w/[\eta]$ stays quite equal to 1.5 mole, and $A_2\overline{M}_w{}^2/\rho^3$ and $[\eta]\overline{M}_w/\rho^3$ increase with increasing molecular weights. For poly-6-methylindene (which may be considered as linear), $A_2\overline{M}_w/[\eta]$ again stays equal to 1.5 mole, and the two other ratios also stay constant.

DTA Study

DTA thermograms were obtained under nitrogen flow on pretreated samples at 120°C for 15 min.

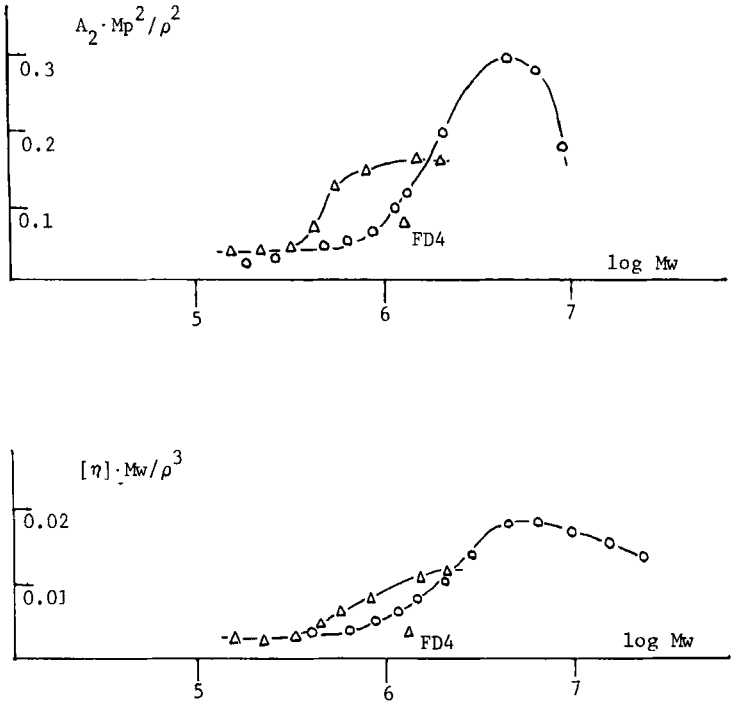

FIG. 12. Variation of two Cassassa ratios with log $\overline{M}_w$: (△) FD; (○) FE.

FD shows an exothermic peak between 200 and 260°C. This peak persists after treatment of FD with boiling ethanol, but it disappears when the thermogram is recorded after a first rise of the temperature to 300°C, which is below the melting-degradation point. We therefore notice a change in the slope at 150°C (Fig. 13).

The study of the FD fractions confirms these results; on the other hand, the FE fractions do not show the exothermic peak for the highest molecular weights.

We think that the exothermic peak could be the result of a post-polymerization reaction of the residual ethylenic bonds, and we attribute the change of the slope, which is reversible, to the transition point.

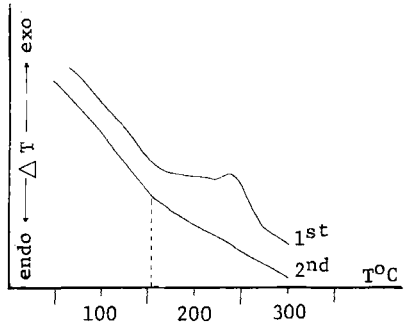

FIG. 13. DTA of sample FD (two successive raises in temperature).

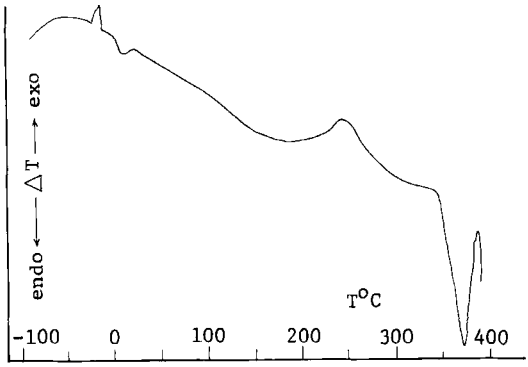

FIG. 14. DTA of sample FD (pretreated at 120°C).

Furthermore a complete study of the thermogram (cf. Fig. 14) shows reversible changes of the structure from -25°C to +25°C and a melting-degradation peak from 345°C.

CONCLUSION

We obtained soluble polymers of bis(1-indenyl) of which the average molecular weights reach 20 millions. The propagation reaction

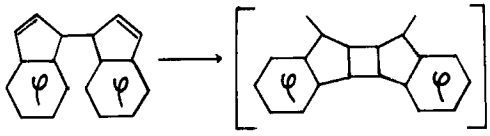

(1)

follows mainly the above "model" equation (1). Such a structure should impart to the polymer a strong rigidity leading to high values of radii of gyration as well as a value of the Mark-Houwink coefficient near unity. We have shown, however, that this is not the case, and physico-chemical aggregates in solution do not seem to exist.

However, we found low, even negative, values of the second virial coefficient. Benzene at 25°C is then practically a theta solvent for polybis(1-indenyl), which explains why the coefficient α is near 0.5. Furthermore important branchings in this polymer were found. This seems sufficient to explain why α is slightly inferior to 0.5, inasmuch as the FD sample, which is more branched overall has the lower α coefficient (0.43 against 0.45 for FE).

We can consider two different models for origin of the branchings. The first one consists of a Friedel-Crafts reaction on a benzene ring of the polymer [Eq. (2)].

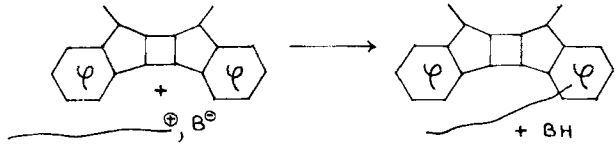

(2)

This model is probable, as was found for example in the case of polymerization of indene and also of 4,7-dimethylindene. The second model is linked to the residual ethylenic bonds in the polymer [Eq. (3)

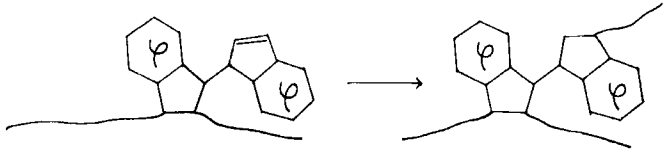

(3)

This model is also highly probable as we have shown that the reaction continues after 100% conversion, leading to increasingly insoluble products.

At first it seems difficult to choose between these two models, but the comparative study of the FD and FE branchings allows an approach to the problem. Both samples show branching, those of FE seeming slightly less important–except for the case of the highest molecular weight fractions; on the other hand, the postpolymerization DTA peak, linked to the residual ethylenic bonds, appears clearly for FD and not for FE. We think that the branching is due mainly to reactions following the first model in the case of FD and to the second model in the case of FE.

This conclusion is also in good agreement with the polymerization conditions. The slightly higher temperature for FD was more favorable to a Friedel-Crafts reaction; conversely, the reaction time, 4 min longer for FE after 100% conversion was reached, was more favorable to the reaction of the still active chains on the ethylenic bonds of the polymer because the latter are no longer in competition with those of the monomer.

We should obtain samples of polybis(1-indenyl) with fewer branches by dropping the polymerization temperature and by stopping the reaction before 100% conversion.

ACKNOWLEDGMENTS

The author is indebted to Prof. Marechal (INSCIR) for reviewing the manuscript.

REFERENCES

[1] E. Marechal, P. Evrard, and P. Sigwalt, Bull. Soc. Chim. France, 1968, 2049.
[2] E. Marechal, P. Evrard, and P. Sigwalt, Bull. Soc. Chim. France, 1969, 1981.
[3] E. Marechal and P. Evrard, Bull. Soc. Chim. France, 1969, 2039.
[4] P. Caillaud, J. M. Huet, and E. Marechal, Bull. Soc. Chim. France, 1970, 1473.
[5] E. Marechal, J. J. Basselier, and P. Sigwalt, Bull. Soc. Chim. France, 1964, 1740.
[6] P. Sigwalt and E. Marechal, Eur. Polym. J., 2, 15 (1966).
[7] P. Sigwalt, J. Polym. Sci., 52, 15 (1961).
[8] P. Nicolet, C. R. Acad. Sci. (Paris), 923C, 282 (1976).

[9] E. Marechal and P. Caillaud, C. R. Acad. Sci. (Paris), 266C, 447 (1968).
[10] J. P. Tortai and E. Marechal, Bull. Soc. Chem. France, 1971, 2684.
[11] G. Leveque, Thèse, Le Mans, France, 1968.
[12] P. Outer, C. I. Carr, and B. H. Zimm, J. Chem. Phys., 18, 830 (1950).
[13] P. D. Cassassa, J. Amer. Chem. Soc., 76, 422 (1954).
[14] H. Garreau and E. Marechal, Eur. Polym. J., 9, 263 (1973).

Accepted by editor June, 7, 1976
Received for publication July 21, 1976